Role of lattice defects on the magnetism of gold nanoparticles irradiated with neutrons

Xiaogang Peng, Long Lin, Louise Stuttgé, Marc Rousseau, Thierry Sauvage, Emilie Voirin, Bertrand Donnio, Mircea V Rastei, Jean-Louis Gallani

Role of lattice defects on the magnetism of gold nanoparticles Irradiated with Neutrons

Xiaogang PENG,[a] Long LIN,[a] Louise STUTTGÉ,[b] Marc ROUSSEAU,[b] Thierry SAUVAGE,[c] Emilie Voirin,[d] Bertrand DONNIO,[d] Mircea V. RASTEI,[d] Jean-Louis GALLANI [d*]

a. Center for Chemistry of Novel and High-Peformance Materials, Department of Chemistry, Zhejiang University, Hangzhou 310027, People's Republic of China.

b. Institut Pluridisciplinaire Hubert Curien, CNRS, Université de Strasbourg, 23 rue du Loess, BP43, 67034 Strasbourg cedex 2, France.

c. Conditions Extrêmes et Matériaux : Haute Température et Irradiation (CEMTHI), CNRS, UPR 3079, Site Cyclotron, 3A rue de la Férollerie, 45071 Orléans cedex 2, France.

d. Institut de Physique et Chimie des Matériaux de Strasbourg, CNRS, Université de Strasbourg, UMR7504, 23 rue du Loess, BP43, 67034 Strasbourg cedex 2, France.

Abstract
The origin of the unexpected magnetic properties of nanoparticles made of gold, silver, or other diamagnetic metals remains obscure despite a large body of experimental and theoretical studies. Whereas many studies have endeavoured at finding correlations between magnetism and nanoparticle size or ligand coating, none so far has attempted at investigating the role of core crystallinity. We have irradiated gold nanoparticles with energetic neutrons or protons with the aim of nucleating lattice defects in the crystalline cores. Comparison of the magnetic behaviours before and after irradiation demonstrates clearly that the presence of defects in the crystalline lattice of the nanoparticles cores contributes efficiently to their magnetism.

Keywords
Nanoparticles ; Magnetism ; Neutrons ; Defects.

Introduction

The question of why noble-metal nanoparticles sometimes display paramagnetism and/or ferromagnetism is still an open one. In spite of many experimental and theoretical work, this behaviour observed in nanoparticles made from metals which are diamagnetic in the bulk is still debated. Many explanations have been brought forth, very often with experimental support : size effect, ligand effect, composition, quantum effects,... but even though the experiments are trustworthy, there is always somewhere another no less trustworthy experimental evidence which hampers a clear interpretation.[1]
One of the major hurdles when investigating macroscopic samples made from many nanoparticles is the lack of reproducibility, a fact which tends to oveshadow all conclusions drawn from the comparison of different samples : no two synthetic batches are identical and within each batch there is an inherent variability of the nanoparticles sizes and structures.[2] Therefore experiments aiming at comparing say, the role of the ligands or the influence of the size are necessarily conducted on different synthetic batches, which adds supplementary uncontrolled parameters and precludes definitive conclusions to be reached.
Most nanoparticles comprise a metal core coated with ligands. The ligands being of molecular nature they are necessarily monodisperse and, in the general case, closed-shell diamagnetic molecules. The core is obviously the most variable ingredient. Its diameter cannot be totally controlled, nor can its exact shape and the number of ligands it bears. Moreover, crystallinity is also poorly -if not at all- controlled.
Within the course of our own experiments we came across the hypothesis that maybe one should consider more closely the consequences of the quality of cores crystallinity on the magnetic properties of such nanoparticles. The feasibility of a high level of control on the crystallinity of silver nanoparticles has recently been demonstrated.[3] Subsequent experiments on single crystalline and multi-twinned silver nanoparticles then showed that the presence of lattice defects in the metal cores tend to render the nanoparticles para- or ferromagnetic.[4] We then devised the procedure described hereafter where energetic particles nucleate lattice defects in the cores, with no chemistry involved.
Direct irradiation of nanoparticles has one great advantage : rather than having to compare nanoparticles coming from different synthetic batches, it becomes possible to synthesize one unique

batch, which is then split in identical aliquots subjected to various experiments, the initial condition remaining identical. We turned to gold nanoparticles as gold is largely unsensitive to oxidation and also has a large enough neutron scatering cross-section which increases the chances to induce defects. Our approach was conforted by a report on the emergence of magnetic moments in plutonium from α-particle decay[5] and another study observing the increase of ferromagnetic properties of palladium nanoparticles (5-10nm diameter) irradiated by swift Au ions.[6]

Materials and methods

Gold nanoparticles have been synthesized in one batch according to a published procedure.[7] After synthesis the oleylamine ligands were exchanged for dodecanethiol ones following standard procedures. Gold has been chosen for its greater chemical stability as compared to *e.g*. silver. Mean diameter of the cores was 6.0nm, with a size dispersion of ±0.4nm, each nanoparticle comprising *ca*. 6700 atoms. An approximate "molecular weight" for the coated nanoparticles would be 1.4×10^6g/Mol. Electronic configuration of gold is [Xe]$4f^{14}5d^{10}6s^1$. We synthesized a large unique batch of gold nanoparticles (1 gram) which was magnetically characterized and then split in 6 aliquots. Four of them were used for neutron irradiation, one for proton irradiation and one was kept untouched (labelled PRIST).

Proton irradiation has been performed using protons at CEMHTI (pelletron accelerator). Energy was set to 2.9MeV, beam current was 4µA and integral number of proton estimated around 1.53×10^{18} protons/cm^2. A 4µm thick layer of nanoparticles was spread on a water-cooled copper block and covered with a 21µm thick copper foil. This sample thickness was chosen so that the Bragg peak fell outside the sample ensuring a more homogeneous irradiation, at the cost of reduced efficiency. After this copper foil the protons energy was down to 1.5MeV, still high enough to generate defects. In spite of the active cooling the temperature of the sample rose to *ca*. 140°C. Thermogravimetric analysis of the original synthetic batch showed that the nanoparticles were thermally stable up to this temperature (see ESI). This sample is labelled PROT.

Neutron irradiation has been performed at the SINQ source of the Paul Scherrer Institute. Source flux is ~10^{14} n/cm^2/s. Four samples labelled NEUTR1, NEUTR 2, NEUTR 3 and NEUTR 4 have been irradiated with thermal neutrons (0.025eV) and received respectively an integral dose of 7.69×10^{15}, 3.12×10^{16}, 3.12×10^{17} and 2.50×10^{18} neutrons/cm^2. Average sample weight was 50mg, most of this mass comes from Au atoms. We therefore had *ca*. 1.5×10^{20} gold atoms subjected to irradiation in each sample. As irradiation led to activation of the samples SQUID magnetometry was performed only after the radioactivity had sufficiently decayed (~1 month). Samples were sealed under vacuum in fused silica tubes. During irradiation temperature of the samples could rise slowly up to *ca*. 85°C (once again within the stability region) due to environmental conditions in the sample chamber.

Magnetometry has been performed with a Quantum Design MPMS SQUID magnetometer. The apparatus has been properly calibrated and checked for artifacts. A small amount of each sample (*ca.* 20mg) was set into a gelatin holder, placed inside a plastic straw. Magnetic response of an empty gelatin holder placed inside an identical straw has been measured as purely diamagnetic and the resulting small magnetic moment has been considered when analyzing the behaviour of the various NPs. No correction for the diamagnetism of the ligand shell of the NPs was applied to the measured values, all curves given here are raw data. In any case the ligands represent at most 8% of the total mass. Magnetization curves have been recorded at room temperature and at 4K. The total magnetic moment measured by the SQUID has been systematically divided by the total mass of the sample (since the mass of the magnetic fraction of the sample is impossible to know), yielding the (mass) magnetization given in the figures. Depending on each sample and its magnetic history, the first magnetization branch of the magnetization curves is not always seen or, when seen, does not always start at the origin. Given the amorphous nature of the samples (no orientational or positional order) this bears no significance.

Transmission Electron microscopy (TEM) was performed on a TOPCON LaB_6 microscope from JEOL.

Results

In order to assess the impact of irradiation on the crystalline structure, electron microscopy has first been performed. As the original gold nanoparticles were a mix of monocrystalline and multi-twinned ones, the outcome of these observations was not expected to be obvious. After thoroughly scanning several microscopy grids we became convinced that the most visible change was that some of the nanoparticles were distorted ot had fused together. Radiation-induced agglomeration and increase of the size has also been reported for irradiated Pd nanoparticles.[6] Figure 1 is an example of two typical images of the non-irradiated sample (PRIST), the most magnetic neutron-irradiated sample (NEUTR4)

and the proton-irradiated sample (PROT). Even though lattice defects are already present in the original sample (green arrows), nanoparticles subjected to high doses of irradiation show clear signs of fusioning and shape altering. This is quite obvious in the picture of proton-irradiated particles which also displays an increased number of defects. More images for all samples are given in ESI.

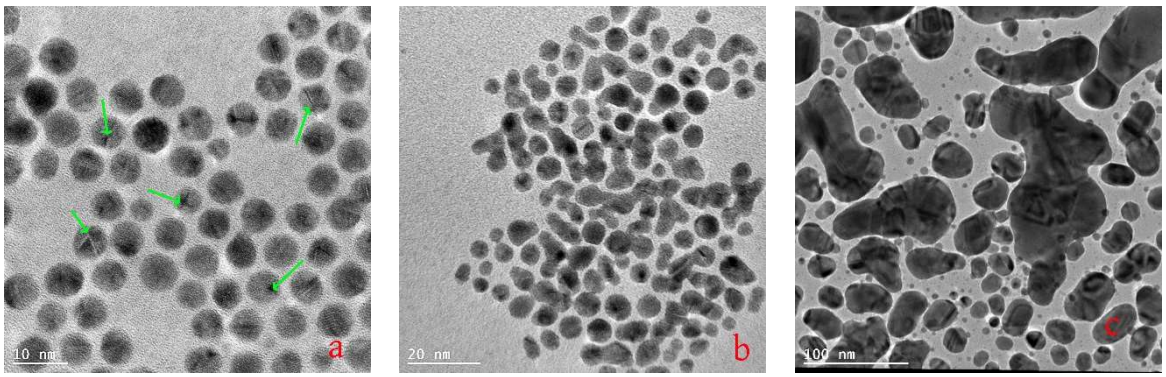

Figure 1. TEM images of non-irradiated nanoparticles PRIST (a) and neutron-irradiated nanoparticles NEUTR4 (b). Lattice defects are already present in the non-irradiated sample (green arrows indicate a few). Note how the shape of some nanoparticles has become less spherical and that some nanoparticles seem to have fused together after irradiation. High energy protons have had a much more visible effect, as seen on the right-hand picture (c).

Sample PROT visibly stands out and probably does not deserve much of a discussion as its structure has been significantly altered, not to say destroyed. Many nanoparticules have fusioned, shapes are irregular, major lattice defects are clearly visible and numerous. On the contrary, neutron-irradiated samples have retained their essential features, the most visible difference being the altered shape of some nanoparticles and their fusion in shapeless clusters. Many nanoparticles resemble much the original ones, it seems difficult to assess the exact nature (screw, edge, vacancy, interstitial...) or number of the lattice defects which are visible. It would also be difficult to unambiguously claim that there are more vacancies or interstitials atoms. We will not comment more on the pictures and turn to the magnetic properties of the samples.

All samples have been magnetically characterized by recording their magnetization *vs*. applied magnetic field at 300K and 4K. Figure 2 compares the magnetization curves recorded at 300K for the non-irradiated sample (PRIST) and the proton-irradiated one (PROT). Figure 3 compares those of neutron-irradiated sample. Details of the low-field region at 300K and magnetization curves at 4K for all samples are given in ESI.

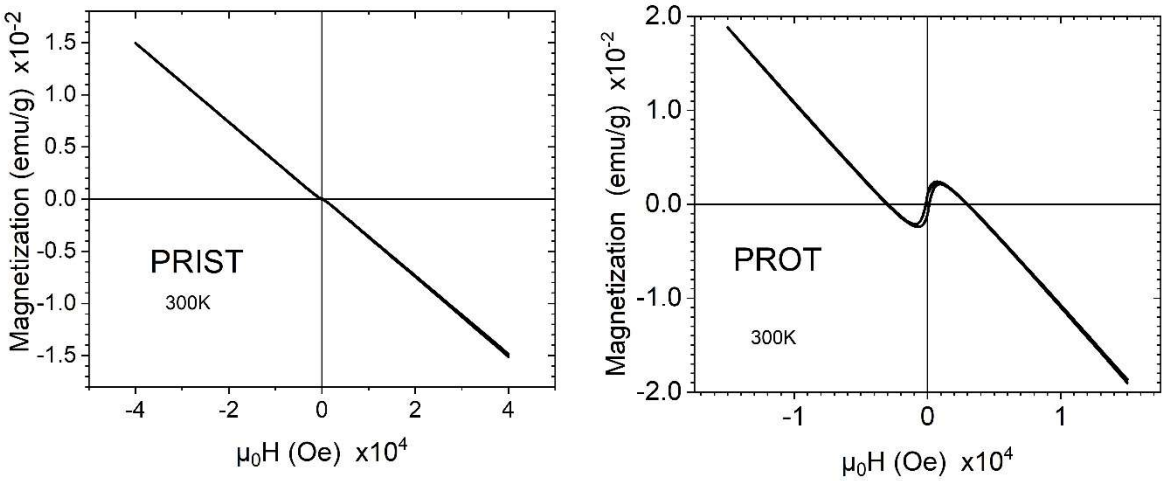

Figure 2. Magnetization *vs*. applied field of non-irradiated sample PRIST (left) and proton-irradiated sample PROT (right).

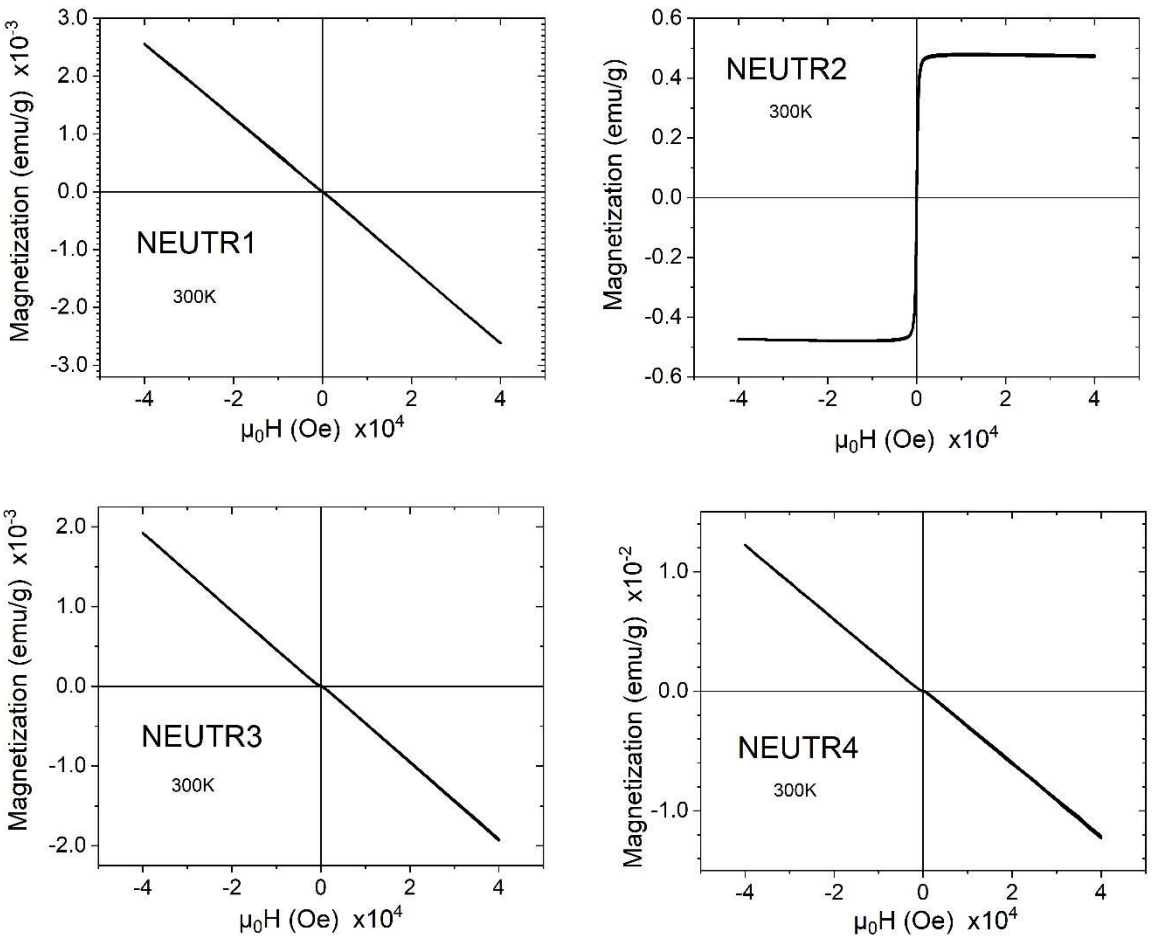

Figure 3. Magnetization *vs*. applied field of : neutron-irradiated samples at 300K.

The non-irradiated sample displays a quasi-diamagnetic behaviour, with only a sliver of ferromagnetism at very low fields, which we reckon is due to the defects inherently present in the metal cores with any synthesis procedure and not to impurities. Possible SQUID artefacts have been looked for and excluded. A clear deviation from this behaviour can then be seen with the irradiated samples PROT (Fig. 2) and NEUTR2 (Fig. 3). Magnetization curves of samples NEUTR1, NEUTR3 and NEUTR4 do not differ much from that of the non-irradiated sample.

Discussion

We aimed to create lattice defaults such as vacancies, interstitial atoms, dislocation loops or stacking faults using only physical means, *i.e.* no chemistry involved and, as much as possible, without altering the samples in any other way. Nucleation of defects in irradiated materials is a known fact,[8] it is actually one of the main causes of concern in nuclear plants.[9] Speaking of nuclear plants, it is interesting to observe that contrary to what we report here, the magnetism of the steel of the reactor pressure vessels is seen to diminish upon neutron irradiation.[10] This is due to the huge difference in structural damage occuring in such high neutron fluxes and, obviously, to the initially much different magnetic properties of the materials, dia- versus para-magnetic.

Nanoparticles submitted to energetic irradiation behave differently than macroscopic samples (as it probably should be expected) because of their limited size and high surface-to-volume ratio. Quoted from reference **11** : "*Instead of diffusing into organized defect structures, the generated point defects tend to annihilate at the particle surface, or material is ejected from the particle volume, as a result of the energetic collision. This can drastically alter the shape of individual particles and cause agglomeration of closely spaced particle groupings.*" The change of shape and sintering of Au nanoparticles under an energetic electron beam has indeed been reported.[12] Proton irradiation certainly produces similar effects and in the case of our neutron irradiated nanoparticles some sputtering has indeed taken place, since the inner side of the fused silica vials which contained the sample came out slightly gold coloured (see ESI).

Let us first consider neutrons. Neutrons and solid metals can interact in two ways : radiative capture or scattering. In the case of gold, capture reactions are the most probable event and they indeed occurred since our samples became radioactive after irradiation.[13] Taking a neutron absorption cross section of approximatively 100 barn,[14] with a source flux of 10^{14} *n*/cm^2/s, one can expect *at the most* ~1.5×10^{12} atoms hit (neutron capture) per second. Similarly, the scattering cross section is approximatively 7b resulting in ~10^{11} atoms hit (neutron scattering) per second. These figures, to be taken with caution, result in a maximum of ~10^{14} hits for sample NEUTR1 and ~10^{17} hits for sample NEUTR4. In addition to the absorption and scattering of neutrons by the gold atoms, some scattering is also expected from interactions with hydrogen atoms (cross-section of *ca*. 80b) in the ligands. This will obviously not result in the nucleation of lattice defects but may induce some damage to the ligands. Other elements (C, S, O) will barely interact with thermal neutrons.
Our samples were irradiated with thermal neutrons (0.025eV) and energy formation of a vacancy in gold is estimated at 0.67eV,[15] meaning that direct knock-on between a neutron and a gold atom cannot result in the formation of a stable vacancy. The neutron absorption cross section is more than ten times that of the scattering cross section, making it then the most probable mechanism. Upon neutron capture a ^{197}Au atom evolves towards an unstable ^{198}Au atom which decays over 2.6 days into ^{198}Hg by emission of 960keV electron. The ^{198}Au then recoils with an energy of 2.85eV, larger than the aforementioned energy for creating a lattice vacancy in gold. This recoiling atom is responsible for the defects appearing in the nanoparticles irradiated with thermal neutrons. Of course, most of the time the recoil does not create a lattice defect but the exact proportion of efficient hits is difficult to estimate. The temperature to which samples were subjected during irradiation (85°C) may have had a two-pronged catalytic effect. On the first hand, temperature may help the sintering of NPs since the fusion temperature of Au nanoparticles becomes close to 300K as their diameter is reduced, this sintering being possibly facilitated by the degradation of the ligands.[16] On the other hand, the temperature much certainly helps the created defects to anneal, hence reduces their number. The important subject of defects annealing will be discussed hereafter.

Protons almost have the same mass as neutrons but are positively charged, therefore Coulomb interactions considerably enhance their interaction with matter. Contrary to neutrons, protons will only be scattered and not absorbed. In large solid samples irradiated with fast particles or ions, the so-called Primary Knock-on Atom (PKA) recoils after the shock and, thanks to its electric neutrality, is able to travel over large distances while disrupting the crystalline lattice and generating defects such as vacancies and dislocation loops. Many of these defects (~70%) either recombine or anneal very rapidly (~ps) yet many stable lattice defects are produced during the course of irradiation, quantified by the DPA (displacement per atom).[17] Estimating the DPA is not an easy task as it depends on many parameters but several models[17] and simulation softwares[18] exist for all kinds of ions and particles. In our case the peak of the Bragg curve is expected to occur at a depth of *ca*. 10µm in solid gold, experimental conditions were therefore set before this peak, ensuring that the sample was more or less homogeneously irradiated throughout its thickness. Under our experimental conditions the average DPA should be around 0.1, we underline it should only be seen as an approximation. All tables and softwares designed for the assessment of radiation damage are intended for use on massive "macroscopic" materials and we are dealing here with heterogeneous particulate materials and nanostructured materials are expected to behave differently.[19,20] It was therefore a bit pointless to try optimizing the irradiation conditions for our systems as the maximum length a collided atom can travel is obviously limited by the diameter of the nanoparticles.

Looking now at the magnetic properties of our neutron-irradiated samples, we reckon that irradiation dose of NEUTR1 was not high enough to produce magnetically significant changes. On the contrary NEUTR4 was too altered (especially the organic ligands) by a very long irradiation, as it received the highest dose of all samples.[21] Sample NEUTR3 is maybe more puzzling since it came out with basically unchanged magnetic properties as compared to NEUTR1, in striking difference with NEUTR2, even though it received ten times more neutrons. A first reason to that could be that due to the intrinsically statistical nature of the experimental process, there is unavoidably some variability from sample to sample, the defects created in the core differing in number and coupling from sample to sample. An illustration of that could probably be the magnetization curves recorded at 4K (ESI), with $M(H)$ of NEUTR1 deviating much more diamagnetism than $M(H)$ of PRIST and NEUTR3. Alternatively, it is also possible that in spite of the longer irradiation times, no so many stable defects were generated in sample NEUTR3 or that their magnetic moments were smaller or less coupled than those created in NEUTR2.

The question of the annealing of the defects is worth considering. Two opposing mechanisms are constantly at play : radioactive decay which introduces defects, and thermal annealing which tends to remove damage. Authors of reference **5** report that thermal annealing of their sample at 300K restores its original magnetic state, the recovery process starting to take effect at temperatures as low as 30K for plutonium. Damage was accumulated for several weeks at 5K but duration of the annealing at various temperatures is not given. While providing useful insight, these experiments cannot be readily compared with ours since our irradiation time was shorter and did not take place at cryogenic temperatures. One last comment regarding the spontaneous annealing of defects has to be made. As our samples became radioactive after irradiation we had to wait several weeks before they could be shipped to us and be handled. This unavoidable lapse of time did not allow us to analyze our results in a similar way -nor as rapidly- as the authors of reference **5**. Still, we believe that the same mechanisms are acting and that in our case, because of the higher temperatures (up to 385K), the production of defects will peak at a certain time before decreasing and tending to a plateau. Based on these considerations we suggest a phenomenological model where defects are exponentially created and annealed via an Arrhenius process. We emphasize that this model is purely *ad hoc* and presented here as a simpler way to explain why the magnetization curve $M(H)$ of some neutron-irradiated samples came out with more drastic changes than others. The evolution rate for the population of defects can be described by the following equation (see ESI for details):

$$\frac{dn}{n} = \left(\frac{n_{max}}{\tau_c} e^{-t/\tau_c} - A e^{E_a/T(t)k_B} \right) dt \qquad (1)$$

which numerical integration results in the curve given in figure 4 :

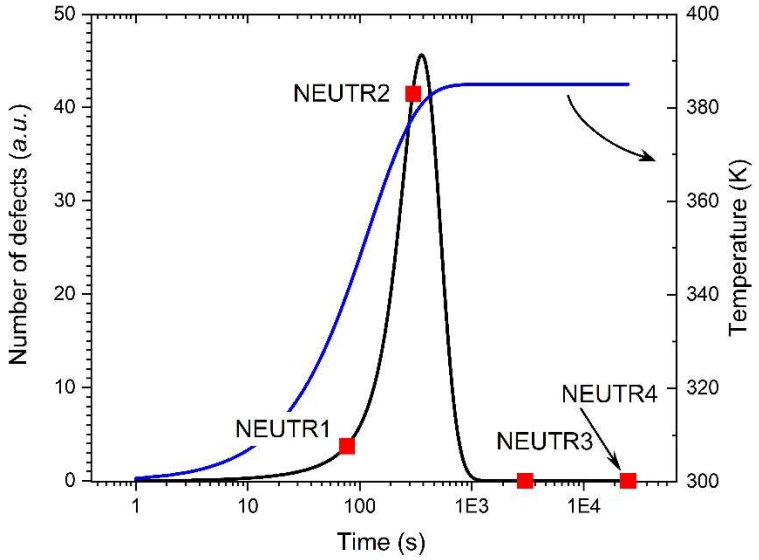

Figure 4. Modelling of the number of stable defects *vs*. time. Red symbols have been placed at the respective irradiation duration of the samples. Y-axis scale is meaningless, this is not a fit. Sumperimposed is the variation of temperature *vs*. time, at the same timescale (blue curve).

If we make the approximation that the magnetization is proportional to the number of stable defects within a sample we can understand the results returned by the magnetic characterization. Sample NEUTR1 has not been irradiated long enough (*ca.* 70s), NEUTR2 has been sufficiently irradiated (*ca*. 300s) but annealing did not proceed efficiently because the temperature did not rise much above 300K. Samples NEUTR3 and NEUTR4, irradiated respectively for *ca*. 3×10^3s and 3×10^4s, spent long enough time at 385K for all defects to anneal and therefore returned to their original magnetic state, with the ligands of NEUTR4 being possibly too damaged.

Low temperature behaviour of all samples (ESI) was essentially identical to what was observed at 300K. With a very narrow (~35Oe) opening of the hysteresis cycle and low remnant magnetization, sample NEUTR2 behaves like a soft ferromagnet, the magnetization saturating at a field of *ca*. 3000Oe. Given the size of the nanoparticles, this saturation value of 0.48emu/g corresponds to ~130μB per nanoparticle, averaged over all the nanoparticles. We underline that there is no reason to calculate a magnetization per gold atom as not all atoms bear a moment, only thoses favorably involved in lattice defects, whose number is unknown. Very probably, some nanoparticles will have a moment higher than

the average value while other will have a smaller one or none.The saturation magnetization remains practically constant from 300K to 4K (ESI). Similar observations have been reported for gold and other metals.[1,22,23] This sample therefore consists of a limited (and unknown) number of ferromagnetic nanoparticles. The magnetic moment is localized in a few places and not evenly distributed.[5,4] Thermal behaviour of the magnetization excludes the possibility of a ferromagnetic impurity being present. It has been possible to fit the magnetization curve recorded at 300K with a Brillouin or Langevin function (ESI) but here again, treating the sample as homogeneous makes little sense.

Sample PROT, which has been irradiated with high energy protons, also behaves differently than the original material even if the change is less spectacular than that of NEUTR2.[21] Nevertheless we obviously cannot link with certainty the observed magnetic properties with these fused nanoparticles which are shapeless and much larger than the original ones. Obviously, the annealing process which is acting for the NEUTR samples is unable to recover the extensive damage suffered by the PROT sample, in spite of the higher temperature (140°C). Moreover, the organic ligands lost their integrity which altered the quality of the interparticle electronic insulation. In any case, point defects such as vacancies or insertions suffice for creating spin imbalances and favoring increased magnetic moments. As will be discussed hereafter, we believe that the appearance of magnetism is mostly due to the presence of lattice vacancies and high-energy protons certainly induce much more damage, as clearly seen in the TEM pictures, than just creating vacancies. In any case, irradiation with energetic protons cannot be directly compared with irradiation with thermal neutrons.

As already mentionned in the introduction, many mechanisms have been proffered for explaining the emergence of para- or ferromagnetism in noble metals nanoparticles. Reasons broadly fall in two categories : some effect related to the ligands attached to the surface, or the peculiar role of some surface atoms which dominate over the core atoms of the nanoparticle as its size decreases. Nevertheless, and this being said, materials may also become magnetic upon the presence of defects[24,25]. The first material clearly displaying defect-induced magnetism (DIM) was graphite.[26,27] It has also been demonstrated that proton irradiation triggers ferro- or ferri-magnetism in HOPG.[28] The most known cases of DIM are that of oxides, nitrides and semiconductors. Most of the time, lattice vacancies -sites where the material's stoichiometry is not respected because of a missing oxygen or nitrogen atom- are at the origin of the effect. Thin films and nano-objects (*e.g.* nanoparticles, tubes, ribbons, …) where geometry induces peculiar constraints at edges and surfaces are other examples.[29,30,31,32] Metals may also become magnetic when defects are present. For example, a DFT study has considered the case of stacking faults and twin boundaries in palladium,[33] and experiments have indeed reported the onset of ferromagnetism in twinned Pd nanoparticles.[23] This is interesting but, as commonly stated, "palladium is close to ferromagnetism" so just a little nudge is enough and the authors indeed suggest that an increase of the density of states at the Fermi level is at the origin of the observed ferromagnetism. Another study mentioned earlier reports the emergence of magnetism in plutonium due to the formation of defects by self-emitted alpha particles, with spinless vacancies inducing magnetic moments on the surrounding lattice.[5]

Our hypothesis is that perfect Au nanoparticles would be diamagnetic. We also hypothesize that the atoms around a vacancy acquire a magnetic moment through an increased localization of their 5*d* electrons. A lower coordination favors narrower bands and higher density of states. An increase of the number of unoccupied 5*d* states is also possible. In this case an electron is transferred and trapped at a defect site, therefore generating a local magnetic moment.

We underline that we do not claim here that the presence of defects is the sole origin of the magnetic properties of nanoparticles made from noble metals. Indeed, the magnetic moments born by defects can coexist happily with other mechanisms (*e.g.* surface currents[34] or persistent currents[35]) previously envisioned, and can even reinforce them, contributing to the variegated behaviours that have been reported by many experimenters.

The question of how these moments are coupled and interact magnetically is unfortunately not totally clear. Many possibilities exist[1,3] and analysis of the thermal behaviour of the magnetization should in principle help discriminate. The authors of ref. **5**, for example, report that the susceptibility of their sample, at the first order, follows a Curie-Weiss law and deduce that a Kondo-like behaviour is observed. This is not the case here, as the thermal behaviour of our samples is featureless and the magnetization basically does not vary between 4K and 300K.

Conclusions

The question as to why nanoparticles made from gold and other diamagnetic metals become magnetic most probably cannot be answered simply. After having worked on the subject for some time our opinion now is that there are several co-existing mechanisms at play. This study aimed at observing the impact of core lattice defects on the magnetic properties using only physical means and no chemistry. The results presented here prove that lattice defects such as vacancies very certainly contribute to the emergence of para- and ferromagnetism in gold nanoparticles. It would be very interesting to devise a means of performing magnetometry while irradiating the nanoparticles. Performing irradiation and magnetic characterization on the same site could bring more definitive results. Theoretical insight on the parameters that make ferromagnetism stable up to 300K in such systems would also be welcome.

Conflicts of interest

The autors declare no conflict of interest.

Acknowledgements

MVR, BD and JLG acknowledge funding received from EOARD (FA8655-13-1-3001) and ANR (ANR-14-OHRI-008 ; ANR-12-BS10-00301). The microscopy plateform of IPCMS is acknowledged for providing access to the JEOL LaB_6 microscope. We thank the CIRCé platform and the CEMHTI pelletron for granting us beamtime on their facilities. The magnetometry platform is acknowledged for access to the SQUID magnetometer. A. Vögele at PSI is thanked for his help. L. Joly is thanked for his help with Blender.

---

[1] G. L. Nealon, B. Donnio, R. Greget, J.-P. Kappler, E. Terazzi, J.-L. Gallani, Magnetism in gold nanoparticles, *Nanoscale,* 2012, **4**, 5244-5258.

[2] We do not consider here so-called "atomically precise nanoclusters" clusters $Au_n(SR)_m$ such as $Au_{25}(SR)_{18}$.

[3] L. Lin, M. Chen, H. Qin, X. Peng, Ag Nanocrystals with Nearly Ideal Optical Quality: Synthesis, Growth Mechanism, and Characterizations, *J. Am. Chem. Soc.*, 2018, **140**, 50, 17734-17742.

[4] L. Lin, X. Peng, E. Voirin, B. Donnio, M. V. Rastei, B. Vileno, J.-L. Gallani, Influence of the Crystallinity of Silver Nanoparticles on Their Magnetic Properties, *Helv. Chim. Acta*, 2023, **106**, e202200165.

[5] S.K. McCall, M.J. Fluss, B.W. Chung, M.W. McElfresh, D.D. Jackson, G.F. Champline, Emergent magnetic moments produced by self-damage in plutonium, *PNAS*, 2006, **103**, 46, 17179.

[6] P. K. Kulriya, B. R. Mehta, D. K. Avasthi, D. C. Agarwal, P. Thakur, N. B. Brookes, A. K. Chawla, R. Chandra, Enhancement of ferromagnetism in Pd nanoparticle by swift heavy ion irradiation, *Appl. Phys. Lett*., 2010, **96**, 053103.

[7] S. Peng, Y. Lee, C. Wang, H. Yin, S. Dai, S. Sun, A facile synthesis of monodisperse Au nanoparticles and their catalysis of CO oxidation, *Nano Res*, 2008, **1**, 229 234

[8] C. Lemaignan, 2010. Nuclear Materials and Irradiation Effects. In: Cacuci, D.G. (eds) *Handbook of Nuclear Engineering*. Springer, Boston, MA.

[9] W. Hoffelner, Damage assessment in structural metallic materials for advanced nuclear plants, *J. Mater. Sci*., 2010, **45**, 9, 2247-2257.

[10] J. Wang, W. Qiang, C. Li, Y. Huang, G. Shu, Y. Zheng, Study of the magnetization work of RPV steel in dependence on neutron irradiation, J. Mag. Mag. Mater., 2021, 537, 168239. And references therein.

[11] S. A. Briggs, K. Hattar, Evolution of Gold Nanoparticles in Radiation Environments. Appearing in : Rahman, M., & Mohammed Asiri, A. (Eds.). (2019). *Gold Nanoparticles - Reaching New Heights*. Available at : http://dx.doi.org/10.5772/intechopen.80366

[12] Yu Chen, R.E. Palmer, J.P. Wilcoxon, Sintering of passivated gold nanoparticles under the electron beam, *Langmuir,* 2006, **22**, 6, 2851–2855.

[13] Au nanoparticles have been found to become efficient radio-sensitizers upon neutron irradiation. E. H. Kim, M.-S. Kim, H. S. Song, S. H. Yoo, S. S., K. Chung, J. Sung, Y. K. Jeong, Y. H. Jo, M. Yoon, Gold nanoparticles as a potent radiosensitizer in neutron therapy, *Oncotarget*, 2017, **8**, 68, 112390–112400.

[14] https://www.ncnr.nist.gov/resources/n-lengths/elements/au.html

[15] C.J. Meechan, R.R. Eggleston, Bildungsenergien von leerstellen in kupfer und gold, *Acta Metallurgica*, 1954, **2**, 680-683.

[16] Ph. Buffat and J.P. Borel, *Phys. Rev. A*, 1976, **13**, 6, 2287.

[17] K. Nordlund, S.J. Zinkle, A.E. Sand , F. Granberg, R.S. Averback, R.E. Stoller, T. Suzudo, L. Malerba, F. Banhart, W.J. Weber, F. Willaime, S.L. Dudarev, D. Simeone, Primary radiation damage: A review of current understanding and models, *J. Nucl. Mat.*, 2018, **512**, 450-479.

[18] For example SRIM, available at http://www.srim.org/

[19] T. T. Järvi, A. Kuronen, and K. Nordlund, K. Albe, Damage production in nanoparticles under light ion irradiation, *Phys. Rev. B*, 2009, **80**, 132101.

[20] I.J. Beyerlein, A. Caro, M.J. Demkowicz, N.A. Mara, A. Misra, and B.P. Uberuaga, Effects of He radiation on cavity distribution and hardness of bulk nanolayered Cu-Nb composites, *Materials Today*, 2016, **16**, 11.

[21] A clear sign that major changes did occur is that samples NEUTR4 and PROT both became unsoluble, contrary to the orignal material and other irradiated samples which all kept their initial solubility and displayed their typical ruby-red colour in solution.

[22] T. Shinohara, T. Sato, T. Taniyama, Surface Ferromagnetism of Pd Fine Particles, *Phys. Rev. Lett*., 2003, **91**, 19, 197201.

[23] B. Sampedro, P. Crespo, A. Hernando, R. Litrán, J. C. Sánchez López, C. López Cartes, A. Fernandez, J. Ramírez, J. González Calbet, M. Vallet, Ferromagnetism in fcc Twinned 2.4 nm Size Pd Nanoparticles, *Phys. Rev. Lett*, **2003**, 91, 237203.

[24] P. Esquinazi, W. Hergert, D. Spemann, A. Setzer, A. Ernst, Defect-Induced Magnetism in Solids, *IEEE Transaction on Magnetics*, 2013, **49**, 8, 4668.

[25] S. P. Gubina, Yu. A. Koksharovb, Yu. V. Ioni, Magnetism of Nanosized "Nonmagnetic" Materials; the Role of Defects (Review), *Russian Journal of Inorganic Chemistry*, **2021**, 66, 1, 1–24.

[26] Y. Kopelevich, P. Esquinazi, J. H. S. Torres, S. Moehlecke, Ferromagnetic- and Superconducting-like Behavior of Graphite, *J. Low Temp. Phys*., **2000**, 119, 691.

[27] P. Esquinazi, A. Setzer, R. Höhne, C. Semmelhack, Y. Kopelevich, D. Spemann, T. Butz, B. Kohlstrunk, M. Lösche, Ferromagnetism in oriented graphite samples, *Phys. Rev. B*, **2002**, 66, 024429.

[28] P. Esquinazi, D. Spemann, R. Höhne, A. Setzer, K.-H. Han, T. Butz, Induced Magnetic Ordering by Proton Irradiation in Graphite, *Phys. Rev. Lett*., **2003**, 91, 227201

[29] I. Lorite, Y. Kumar, P. Esquinazi, C. Zandalazini, S. Perez de Heluani, Detection of Defect-Induced Magnetism in Low-Dimensional ZnO Structures by Magnetophotocurrent, *Small*, 2015, 11, 34, 4403-4407.

[30] A. Sundaresan, C.N.R. Rao, Ferromagnetism as a universal feature of inorganic nanoparticles, *Nano Today*, 2009, **4**, 96-106.

[31] S. Ning, P. Zhan, Q. Xie, WP. Wang, ZJ. Zhang Defects-Driven Ferromagnetism in Undoped Dilute Magnetic Oxides: A Review, *J. Mater. Sci. Techn.,* 2015, **31**, 10, 969.

[32] S. Zhou, X. Chen, Defect-induced magnetism in SiC, *J. Phys. D: Appl. Phys*., 2019, **52**, 393001

[33] S. S. Alexandre, E. Anglada, J. M. Soler, F. Yndurain, Magnetism of two-dimensional defects in Pd: Stacking faults, twin boundaries, and surfaces, *Phys. Rev. B*, 2006, **74**, 054405.

[34] A. Hernando, P. Crespo, M.A. Garcia, E. Fernandez-Pinel, J. de la Venta, A. Fernandez, S. Penades, Giant magnetic anisotropy at the nanoscale: Overcoming the superparamagnetic limit, *Phys. Rev. B.*, 2006, **74**, 052403.

[35] R. Gréget, G. L. Nealon, B. Vileno, P. Turek, C. Mény, F. Ott, A. Derory, E. Voirin, E. Rivière, A. Rogalev, F. Wilhelm, L. Joly, W. Knafo, G. Ballon, E. Terazzi, J.-P. Kappler, B. Donnio, J.-L. Gallani. Magnetic Properties of Gold Nanoparticles: A Room-Temperature Quantum Effect. *ChemPhysChem*, 2012, **13**, 3092-3097.

Electronic Supplementary Information

Role of lattice defects on the magnetism of gold nanoparticles Irradiated with Neutrons

1) Thermogravimetric analysis of sample PRIST.

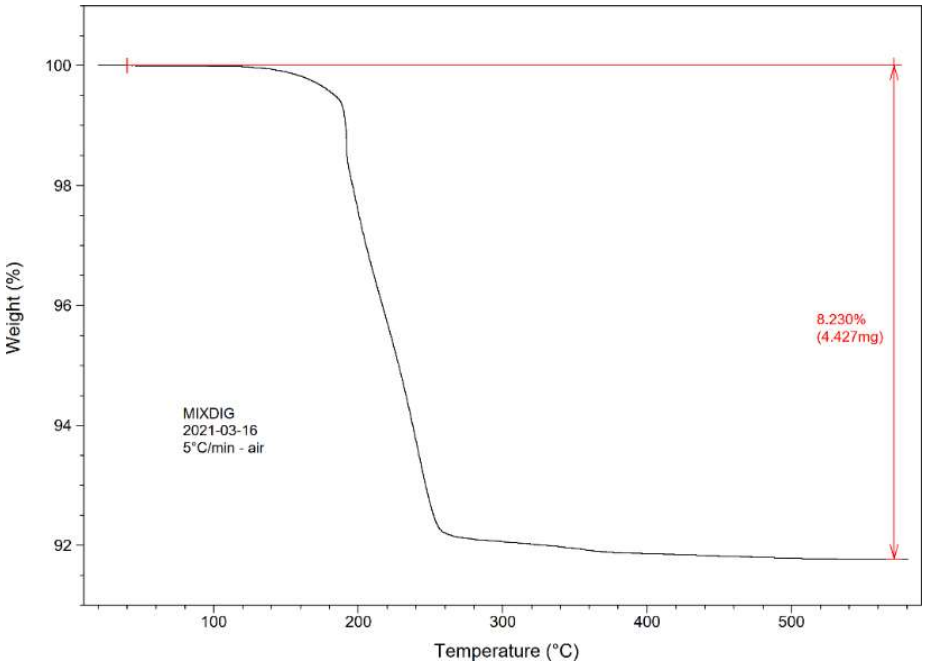

Sample is thermally stable in air up to ~140°C.

With an average diameter of 7nm, the Au nanoparticles have a core weighing *ca.* 3.47×10^{-18}g and a surface of 1.54×10^{-16}m^2. On this surface an estimate number of 900 dodecanethiol ligands are grafted (~0.17nm^2 per ligand), weighing 3.0×10^{-19}g. Supposing that these ligands "burn", the resulting weight loss would represent *ca.* 8%, which is what is observed on the TGA curve : total weight loss 8.23%.

2) Silica tube which contained sample NEUTR4 after irradiation. Note the sputtering of gold on the inner walls.

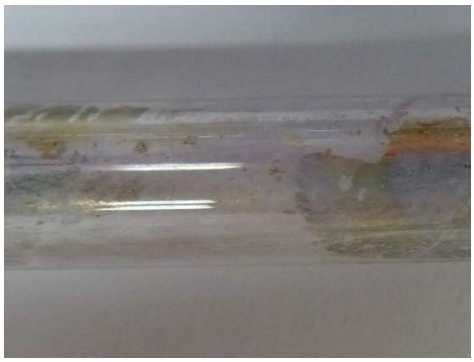

3) Magnetization curves : curves at 4K and details at low field at 300K

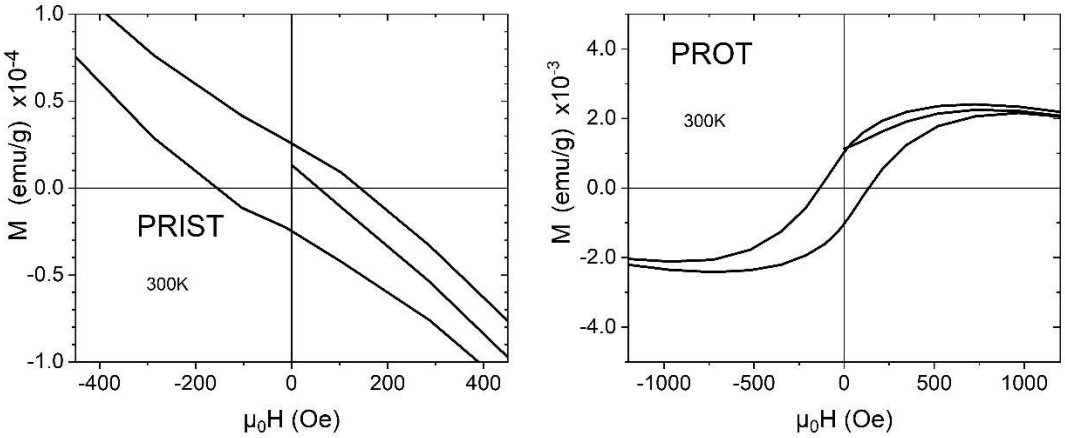

details of the low-field region for samples PRIST and PROT

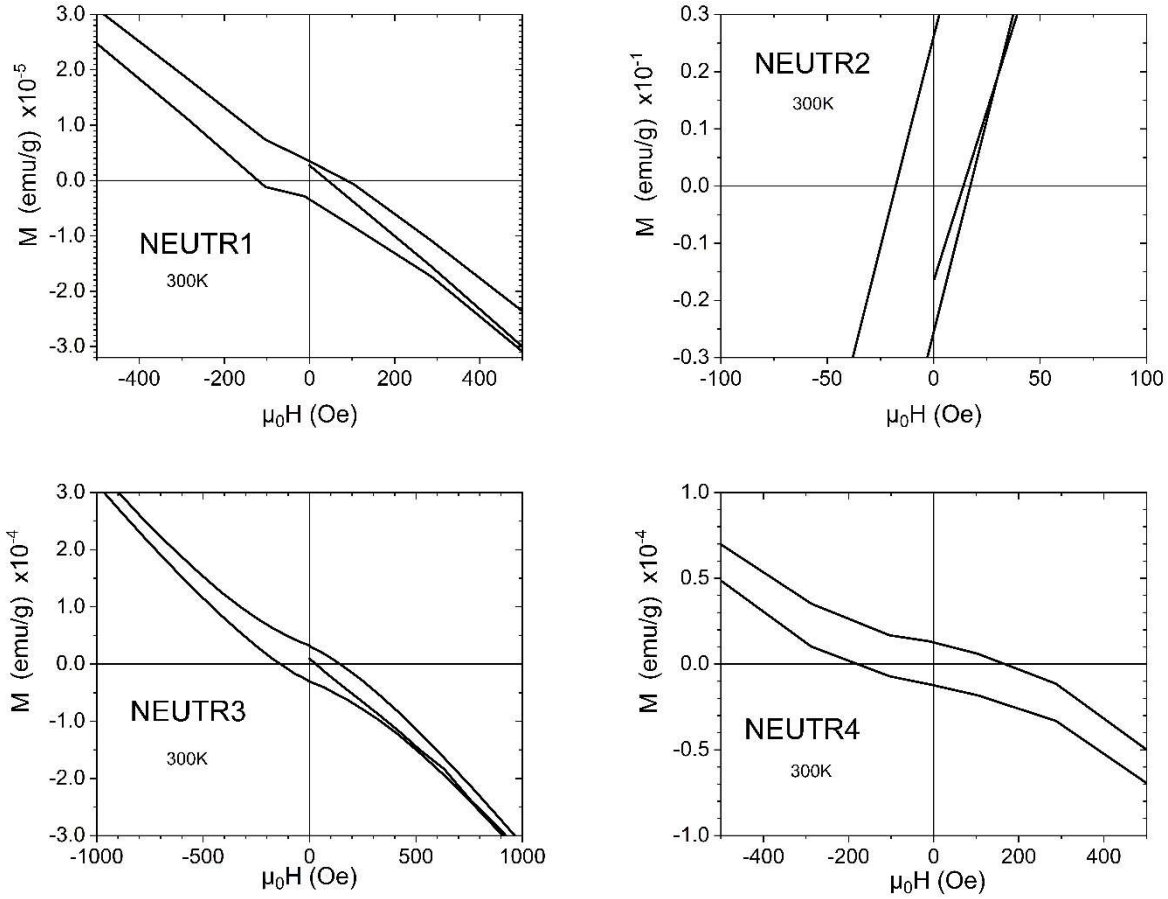

details of the low-field region for neutron-irradiated samples

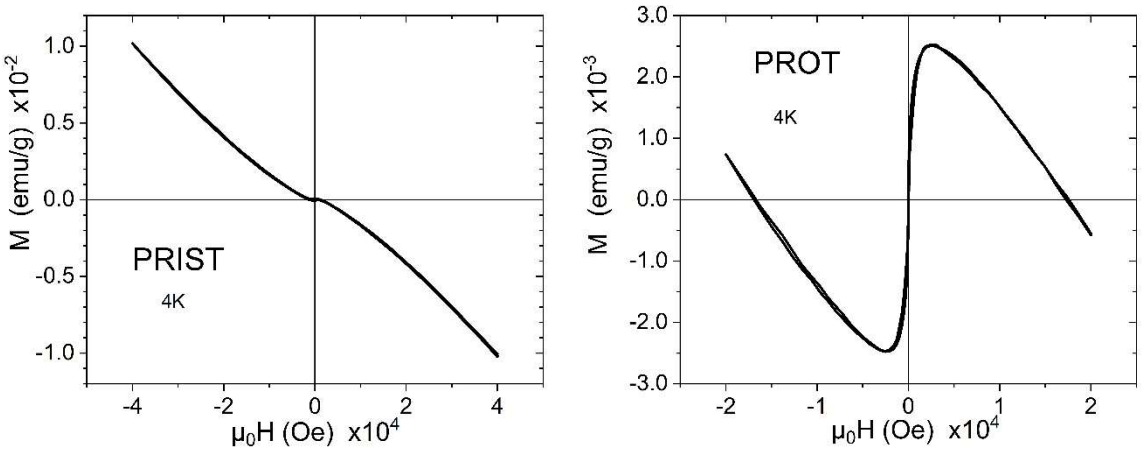

Magnetization curves of samples PRIST and PROT recorded at 4K

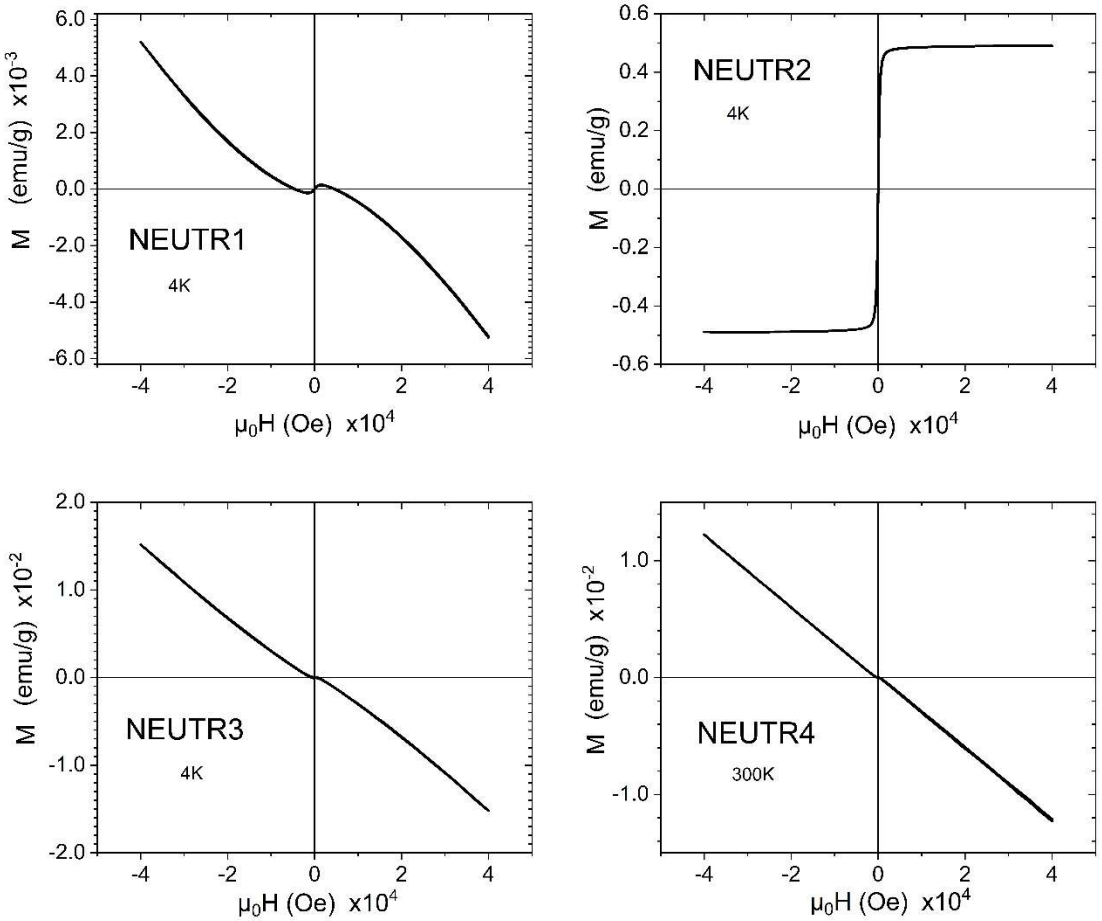

Magnetization curves of neutron-irradiated samples recorded at 4K

4) Thermal behaviour of NEUTR2

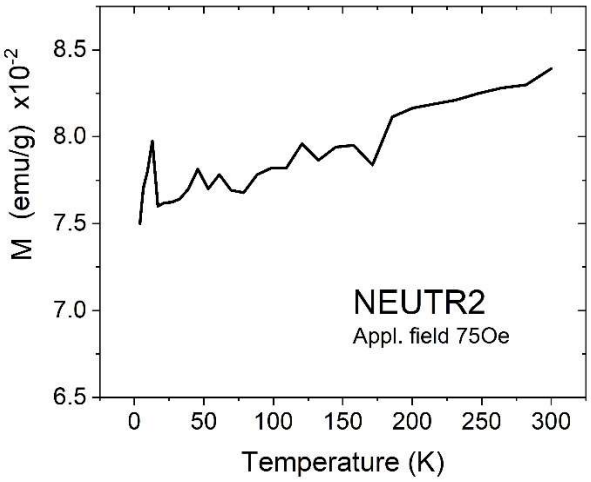

Magnetic moment is almost temperature independant, therefore excluding the possibility of any ferromagnetic impurity.

5) Tentative fit of sample NEUTR2

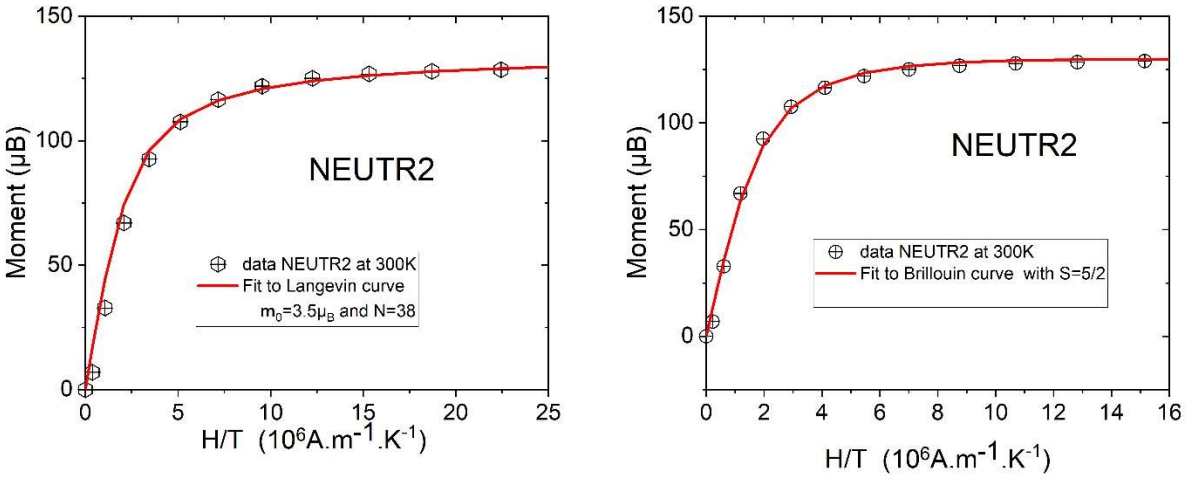

Left : Fit to a Langevin function with an average moment m_0=3.5μ_B and a number of moments N=38.
Right : Fit to a Brillouin curve with S=5/2 and L=0. Total moment M_0=131μ_B.

6) Phenomenological model

We emphasize that this "model" is purely *ad hoc* and is presented here as a simpler way to explain why the magnetization curve of some neutron-irradiated samples came out with more drastic changes than others. We make the crude approximation that the magnetization is proportional to the number *n* of stable defects within a sample.

Following the authors of the reference **5**, as quoted in the main text, we assume that the vacancies are created with an exponential law :

$$\frac{dn_a}{dt} \sim e^{-t/\tau_c} \qquad (1)$$

which gives the rate of vacancies created *vs.* time t, $\tau_c \approx 400s$ a characteristic time related to the activity of ^{198}Au. This rate decreases with time since the number of vacancies that can be created in a given volume is limited by the defect-free volume remaining. Eventually a $n_{\max}$ number of defects will be reached :

$$n(t) = n_{max}(1 - e^{-t/\tau_c}) \qquad (2)$$

Sample temperature T is taken to increase from 300K to 385K in $\tau_T \approx 120s$ (samples are sealed under vacuum which prevents quick thermalization) with a similar law :

$$T(t) = 300 + 85\left(1 - e^{-t/\tau_T}\right) \qquad (3)$$

We underline that temperature was not controlled, its change over times simply comes from the environmental conditions in the experimental chamber. This increase of temperature with time will favor the annealing of the lattice vacancies, thermally activated following an Arrhenius law :

$$k = Ae^{E_a/T(t)k_B} \qquad (4)$$

k the rate of defects annealing, A=6×10^{11}s^{-1} the usual pre-exponetial factor (here the rate of defects annihilation), E_a =1eV the activation energy for the diffusion of a vacancy, k_B the Boltzmann constant. With E_a estimated to be ~1eV, it may seem dubious that 385K would be enough to anneal the defects but authors of ref. **5** (main text) observe that their samples are totally annealed and defectless at 300K (~0.026eV), the annealing process starting to take effect at 30K. Gold is not plutonium but vacancy diffusion energy is roughly the same in most metals (E_a~1.4eV for Pu). Gold temperature of fusion is 1064°C, that of plutonium is 639°C, certainly favoring a quicker thermal annealing.

At a given time t a number $n(t)$ of vacancies are present and therefore the number of defects which become annealed each second is :

$$\frac{dn_a}{dt} = n(t)Ae^{E_a/T(t)k_B} \qquad (5)$$

With these three equations is is possible to built a phenomenological equation which gives the number of defects n in the sample as a function of time t, T being given by equation (3):

$$\frac{dn}{dt} = \frac{n_{max}}{\tau_c}e^{-t/\tau_c} - n(t)Ae^{E_a/T(t)k_B} \qquad (6)$$

which can be rewritten :

$$\frac{dn}{n} = \left(\frac{n_{max}}{\tau_c}e^{-t/\tau_c} - Ae^{E_a/T(t)k_B}\right)dt \qquad (7)$$

which is then numerically integrated, yielding the following curve :

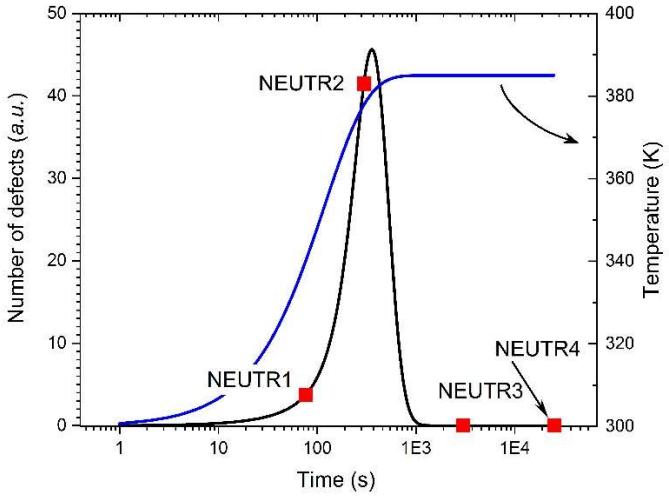

Modelization of the number of stable defects *vs*. time. Red symbols have been placed at the respective irradiation duration of the samples. Y-axis scale is meaningless, this is not a fit, we only wish to illustrate the shape of the curve. Sumperimposed is the variation of temperature vs. time, at the same timescale (blue curve).

The number of defects intially increases with irradiation time but thermal annealing of the lattice vacancies kicks in and reduces the number of defects, until no defects are created anymore. We suggest that this levelling of the effective number of radiation-induced defects, added to the fact that

probably not all created defects bear a magnetic moment, allows to understand why a longer irradiation time does not result in a higher magnetization or, at least, why the magnetization does not saturate at some higher value. By pure chance, sample NEUTR2 has been irradiated with a duration close to the optimum for defects creation. NEUTR1 was irradiated not long enough, in samples NEUTR3 and NEUTR4 the annealing process was fully active and overcame the nucleation process.

7) TEM images of proton and neutron irradiated samples.

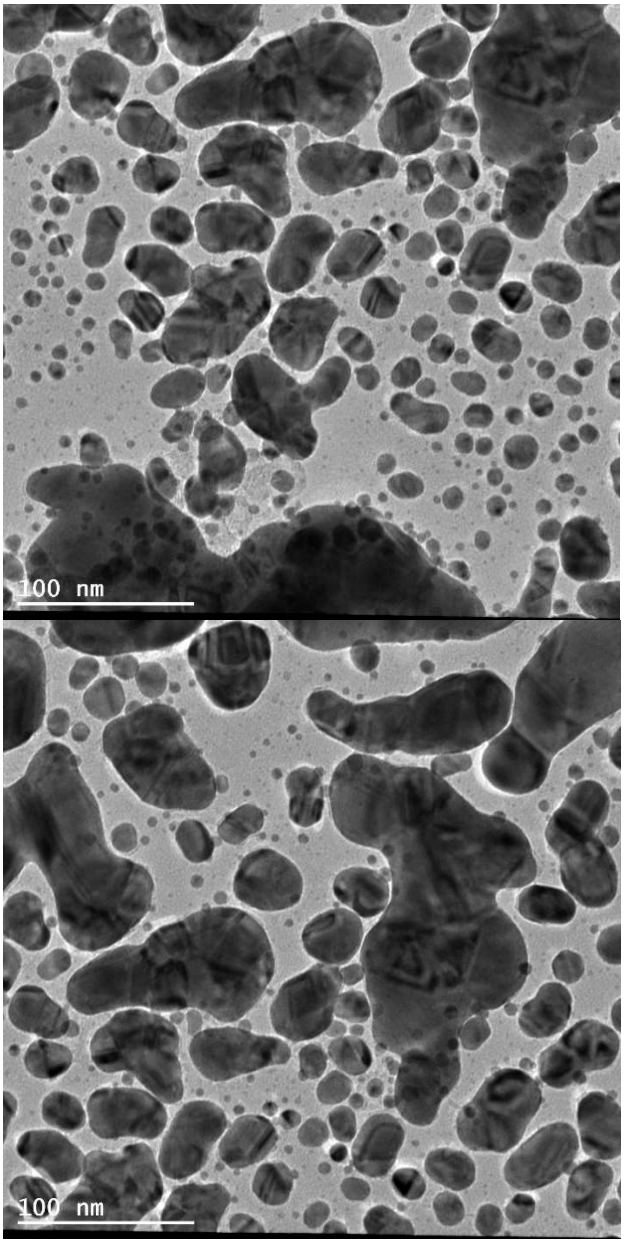

PROT

This sample is the one which seems to have suffered the most damage. In any case, there are much less “surviving” particles in this sample than in the samples which have been hit with neutrons, *e.g*. sample NEUTR4 below. Moreover, the lattices defects are not just vacancies

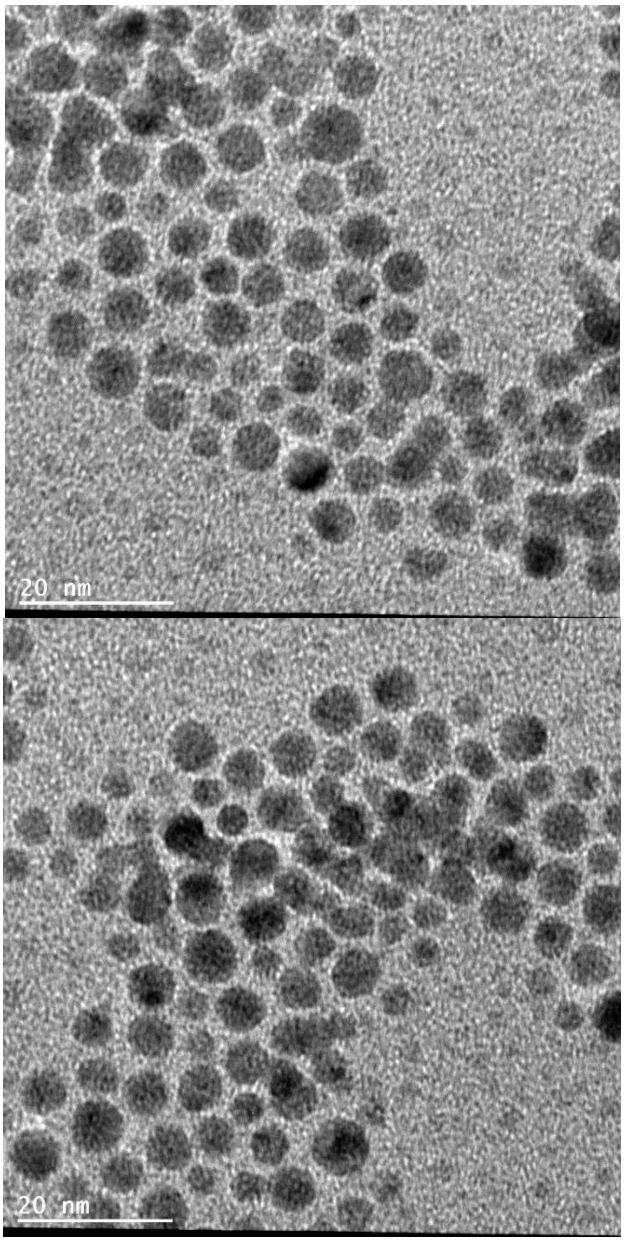

NEUTR1

Almost no changes as compared to the original non-irradiated sample.

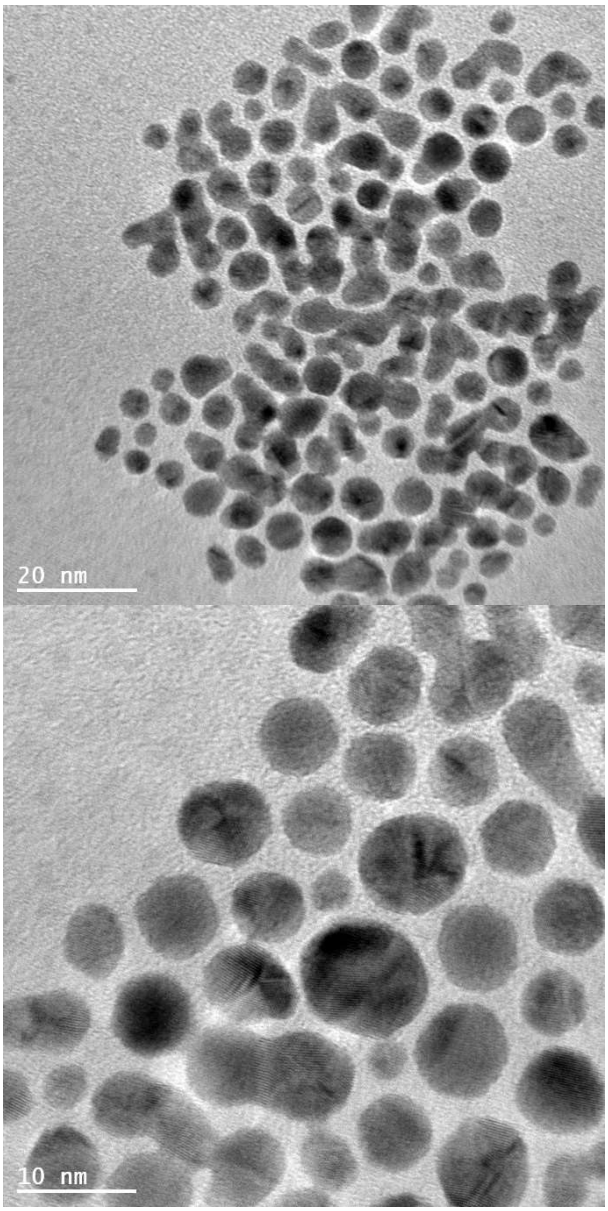

NEUTR2

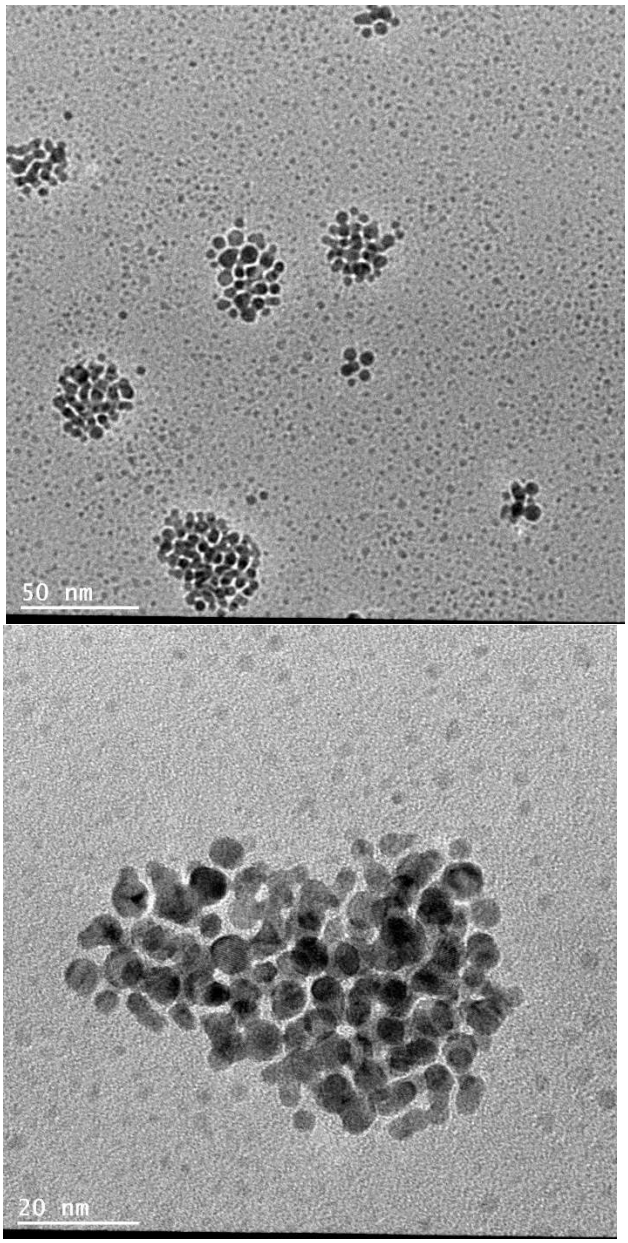

NEUTR3

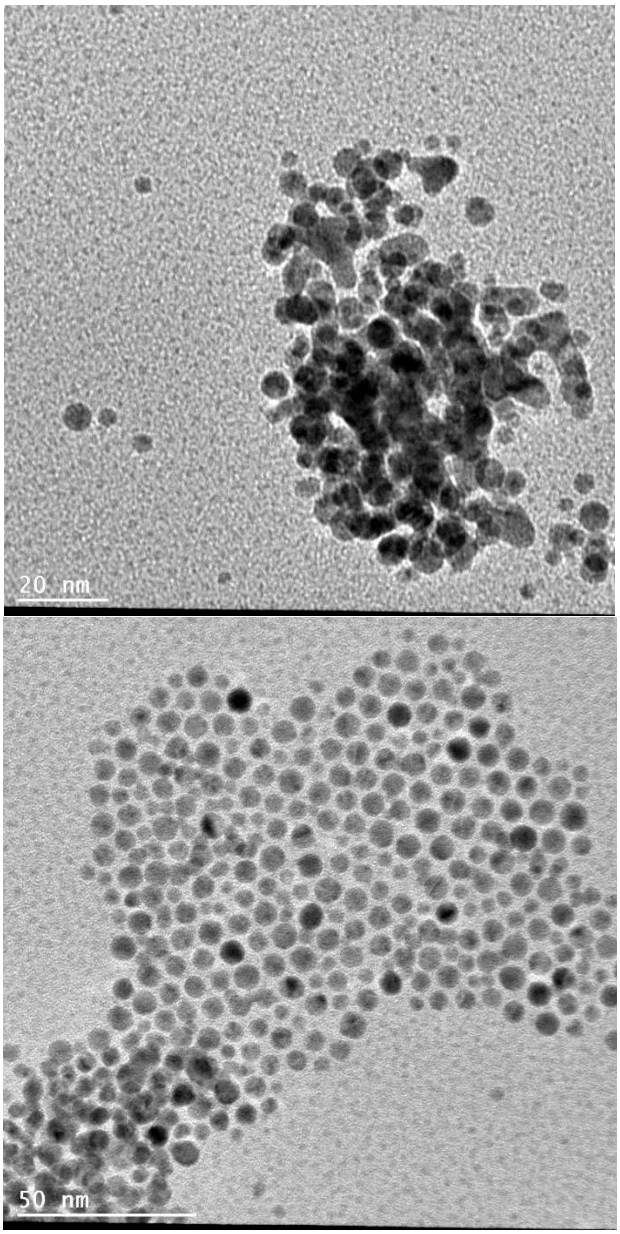

NEUTR4

In spite of the high neutron dose, not all nanoparticles are destroyed (right). Organic ligands probably suffered large damage (sample became unsoluble) but this cannot be assessed with electron microscopy.